CrystEngComm

Accepted Manuscript

ROYAL SOCIETY OF CHEMISTRY

www.rsc.org/crystengcomm

A new ternary ferroelectric crystal of $Pb(Y_{1/2}Nb_{1/2})O_3$-$Pb(Mg_{1/3}Nb_{2/3})O_3$-$PbTiO_3$

Xiuzhi Li, Zujian Wang, Ying Liu, Chao He, Xifa Long*

Key Laboratory of Optoelectronic Materials Chemistry and Physics, Fujian Institute of Research on the Structure of Matter, Chinese Academy of Sciences, Fuzhou, Fujian 350002, China

A ternary piezo-/ferroelectric crystal of $0.22Pb(Y_{1/2}Nb_{1/2})O_3$-$0.44$ $Pb(Mg_{1/3}Nb_{2/3})O_3$-$0.34PbTiO_3$ (PYN-PMN-PT(22/44/34)) with dimensions of 26 × 26 × 10 mm^3 has been grown by the top-seeded solution growth (TSSG) method for the first time with a purpose of exploring new ferroelectric single crystals with high piezoelectric properties, and which was characterized by structural analysis and electrical measurements. The rhombohedral and tetragonal phases co-exist in the as-grown crystals, which belong to the morphotropic phase boundary (MPB) region. The Curie temperature T_C and the rhombohedral-tetragonal phase transition temperature T_{RT} reached 125 ºC and 90 ºC. The dielectric constant ε′, dielectric loss tangent tanδ, piezoelectric coefficient d_{33}, longitudinal electromechanical coupling coefficient k_{33}, remnant polarization P_r and coercive field E_c were found to be 1280 , 0.04, 1344 pC/N, 82%, 21.4μC/cm^2, 3.4 kV/cm, for [001]-oriented crystals at room temperature, respectively. These results show that the PYN-PMN-PT(22/44/34) crystals are a promising candidate for uses in electromechanical transducers for

* Corresponding Author: Phone: (86)-591-83710369; Fax: (86)-591-83714946 Email: lxf@fjirsm.ac.cn

applications.

1. Introduction

$Pb(Mg_{1/3}Nb_{2/3})O_3$-$PbTiO_3$ (PMN-PT) single crystals have attracted much attention due to their high piezoelectric coefficients, large longitudinal electromechanical coupling factors, high dielectric constants, low dielectric losses and exceptionally high strain levels, with compositions close to or within the morphotropic phase boundary (MPB) region in the past years.[1-15] However, there are some drawbacks in this system. The Curie temperature (T_C) of PMN-PT crystals near the MPB range is only about 150 °C, and even lower is the rhombohedral-tetragonal phase transition temperature (T_{RT}) which is about 80°C.[16-17] The low values of these two temperatures make the materials depoled easily, greatly limiting their applications in the high temperature range. Another drawback is the low coercive field (E_c = 2 - 3 kV/cm) of the PMN-PT crystals, which causes the crystals to depole very easily and thereby their piezoelectric performance to degrade, limiting their application in high power field.

More recently, great interest has been paid in introduction of $Pb(B'B'')O_3$ (B' = Yb^{3+}, In^{3+}, Sc^{3+}, ⋯; B" = Nb^{5+}, ⋯) into PMN-PT systems, for example, $Pb(Yb_{1/2}Nb_{1/2})O_3$-$Pb(Mg_{1/3}Nb_{2/3})O_3$-$PbTiO_3$ (PYbN-PMN-PT),[18-19] $Pb(Sc_{1/2}Nb_{1/2})O_3$-$Pb(Mg_{1/3}Nb_{2/3})O_3$-$PbTiO_3$ (PSN-PMN-PT),[20] and $Pb(In_{1/2}Nb_{1/2})O_3$-$Pb(Mg_{1/3}Nb_{2/3})O_3$-$PbTiO_3$ (PIN-PMN-PT),[21-25] which show promising piezoelectric properties and a higher Curie temperature.

The structure of the $Pb(Y_{1/2}Nb_{1/2})O_3$(PYN) belongs to complex perovskite ABO_3 family with Y^{3+} and Nb^{5+} ordered on the B-site. It is reported that PYN has a

pseudo-monoclinic antiferroelectric phase at room temperature, and varied to paraelectric phase at around 342 ºC.[26-27] Therefore, great interest has been paid in PYN as an end member in $Pb(Zn_{1/3}Nb_{2/3})O_3$-$PbTiO_3$ (PZT) in order to improve the ferroelectric and piezoelectric properties.[28-29] We believe that PYN can form a solid solution with PMN-PT, which should present an MPB and exhibit good electric properties compared with the PMN-PT crystals. In this work, the crystal of PMN-PT doped with PYN was grown by the top-seeded solution growth method for the first time and the ferroelectric and piezoelectric properties were characterized.

2. Experiments

2.1 Crystal growth

The PYN-PMN-PT single crystals were grown by the TSSG method. The starting chemicals, PbO (99.99%), TiO_2 (99.90%), MgO (99.90%), Nb_2O_5 (99.90%), Y_2O_3 (99.99%) and H_3BO_3 (99.90%), were weighed according to the stoichiometric composition of 0.22PYN-0.44PMN-0.34PT (PYN-PMN-PT(22/44/34)). A mixture of PbO and H_3BO_3 (with a molar ratio of PbO:H_3BO_3 = 5:1) was used as high-temperature solution. A flux to solute molar ratio of 5:1 was used. The mixed chemicals were heated to 1050 ºC at a rate of 100 ºC/h in a Pt crucible with a size of $\Phi 60 \times 55$ mm^2 in a vertical tubular furnace, and then slowly cooled down from 1050 ºC to 900 ºC with a Pt wire was used as seed at a rate between 0.5 and 2 ºC/h. At the last stage, the grown crystal was pulled out of the melt surface and then cooled down to room temperature at a rate of 20 ºC/h. Finally, PYN-PMN-PT(22/44/34) polycrystal

was obtained, as shown in Fig. 1a.

Then, a small $[001]_{cub}$-oriented PYN-PMN-PT single crystal cutting from the grown polycrystal was used as seed and the saturation temperature of the solution was determined accurately by repeated seeding trials. The starting chemicals and the mixture of high-temperature solution were same as above. The crystal growth took place upon cooling from 1020 ºC to 920 ºC at a rate of 0.2 ºC/h. At the end of a slow cooling process, the grown crystal was pulled out of the melt surface and then cooled down to room temperature at a rate of 20 ºC/h. A brown quadrate single crystal with dimensions of 26 × 26 × 10 mm^3 was obtained, as show in Fig. 1b.

2.2 Characterization procedure

The structural analysis and sample orientation were performed by means of X-ray diffraction (XRD) at room temperature on a Rigaku diffractometer (Rigaku, Japan) equipped with Cu Kα radiation and a graphite monochromator. The data were collected with a scan step of 0.02° (2θ) and an angular range of 10 - 80°. A polarized light microscope (LV100POL, Nikon, Japan) was employed to determined the phase and electric domain of the as-grown PYN-PMN-PT(22/44/34) crystals. The $[001]_{cub}$-oriented crystal samples were cut from the as-grown crystal (bar and platelet). All the samples were polished and coated with silver paste on the $[001]_{cub}$ faces as electrodes. A platelet sample with dimensions of 2.44×2.98×1.18 mm^3 was used for dielectric, piezoelectric and ferroelectric measurements. For resonance and anti-resonance measurements, a bar sample with dimensions of 1.13×1.28×3.64

mm^3 was prepared. The dielectric constant (ε') and dielectric loss tangent ($tan\delta$) were measured at various frequencies as a function of temperature upon heating from –50 ºC to 300 ºC using a computer-controlled Alpha-A broadband dielectric/impedance spectrometer (Novocontrol GmbH, Germany), with an AC signal of 1V (peak-to-peak) applied. The resonance (f_a) and anti-resonance (f_r) frequencies of the bar sample at different temperature a step of 5 ºC from 20 ºC to 150 ºC as a function of frequencies were measured. Poling was performed by applying a DC electric field of 1kV and 3kV along the [001] direction for the platelet and bar of the crystal respectively at 120 ºC for 15 min, and then keeping the field on while cooling down to room temperature. Piezoelectric coefficient was measured using a quasistatic d_{33} meter (Institute of Acoustics, Chinese Academy of Sciences, model ZJ-4AN). The ferroelectric hysteresis loops were measured using an aix-ACCT TF2000 analyzer (at the frequencies f=2Hz).

3. Results and discussion

3.1 Structural analysis and phase of crystals

Fig. 2 presents the powder XRD pattern for grown PYN-PMN-PT(22/44/34) crystal measured at room temperature, showing a pure perovskite phase. In order to accurately study the structure of PYN-PMN-PT(22/44/34) at room temperature in more detail, special attention was concentrated on the (200) reflections around 2θ = 45°. It is well known that the XRD profiles of the (200) reflections will show only a single peak R(200) in the rhombohedral structure because all the (200) planes share

the same lattice parameters, whereas in the tetragonal phase the (200) reflections should be split into two peaks, the T(200)/(020) and T(002) profiles.[30] As shown in the insets in Fig.2, for PYN-PMN-PT(22/44/34) crystal, the (200) reflection is composed of only one single peak, which corresponds to the rhombohedral or pseudo-cubic phase. The lattice parameters of the single crystals were refined to be a = 4.034 Å and α = 89.956 °, based on the XRD data.

Actually, the XRD profiles of the (200) reflections show a little wider peak, which indicate the existence of the tetragonal phase. A polarized light microscope was employed in order to approve this conclusion. The vibration directions of all the domains in the [001]-oriented plate are practically parallel or perpendicular to each other and the extinction angle θ determined as the smaller angle between the domain's vibration direction and the [100] crystallographic axis is practically the same for all domains, namely, θ =45° in the R phase and θ =0° in the T phase.[31] Fig. 3 shows the electric domain micrographs of the [001]-oriented plate of the PYN-PMN-PT(22/44/34) crystal with a thick of 46μm. When the crossed polar light are in the [100] position as shown in Fig. 3a, the crystal shows some bright regions, labeled for R. The corresponding bright areas appear to be in extinction when θ =45° as shown in Fig. 3b, which indicate the as-grown crystal belongs to rhombohedral symmetry. On the other hand, the black regions in Fig. 3a, labeled for T, become bright when θ =45° in Fig. 3b which indicate the existence of tetragonal symmetry. In conclusion, the rhombohedral and tetragonal phases co-exist in the as-grown crystals, which belong to the morphotropic phase boundary (MPB) region.

3.2 Dielectric Properties

Fig. 4a shows the variations of the dielectric constant (ε′) and dielectric loss tangent (tanδ) of the unpoled [001]-oriented PYN-PMN-PT(22/44/34) crystal sample as a function of temperature at the frequencies of 1 Hz, 100 Hz, 10K Hz and 1000kHz. The maximum of dielectric constant indicates a Curie temperature T_C of 125 ºC (at 10 kHz). In order to determine the rhombohedral-tetragonal phase transition temperature T_{RT} of the crystal, the dielectric constant (ε′) and dielectric loss tangent (tanδ) of the poled platelet sample were measured as the function of the temperature, as shown in Fig. 4b. The dielectric anomaly observed around 90 ºC in Fig. 4b corresponding to the rhombohedral-tetragonal phase transition temperature $T_{R/T}$. The dielectric constant and loss tangent for the poled sample are 1280 and 0.04, respectively, at room temperature.

Furthermore, the dielectric constant shows a relative broad maximum with frequency dispersion, the temperature of which (T_m) shifts to higher temperature with the increasing frequency, indicating typical dielectric relaxor behavior[12,32-33]. In normal ferroelectrics, the temperature dependence of the dielectric constant above the Curie temperature obeys the Curie-Weiss law: $1/\varepsilon' = (T - T_{CW})/C$, where C is the Curie constant and T_{CW} is the Curie-Weiss temperature. However, in relaxor ones, the dependence relation deviates the Curie-Weiss law due to short-range correlations between polar regions.[12,34] In a wide range above T_m and below Burns temperature (T_B), the temperature dependence of 1/ε′ follows the Lorentz-type quadratic

relationship:[35-37]

$$\frac{\varepsilon_A}{\varepsilon'} - 1 = \frac{(T - T_A)^2}{2\delta^2} \quad (1)$$

where T_A and ε_A are the fitting parameters and δ is a measure of the degree of diffuseness of the permittivity peak. Figure 5 shows the temperature dependence of $1/\varepsilon'$ (at 100 kHz) for the grown crystal. It can be seen that the data can be well fitted into the Lorentz-type quadratic relationship with parameters of ε_A = 22506, δ = 50.43 ºC, T_A = 103.50 ºC.

3.3 Electromechanical Coupling and Piezoelectric Properties

In order to determine the electromechanical coupling factor (k_{33}), the resonance (f_r) and antiresonance (f_a) frequencies for the crystal sample at various temperature were measured. The longitudinal electromechanical coupling factor (k_{33}) was derived by the following equation:[38-39]

$$k_{33}^2 = \frac{\pi}{2}\frac{f_r}{f_a}\cot\left(\frac{\pi}{2}\frac{f_r}{f_a}\right) \quad (2)$$

Figure 6 shows the impedance and phase angle as functions of frequency for the PYN-PMN-PT(22/44/34) single crystal at the temperature of 55 ^{o}C. It can be seen that impedance spectrum shows two peaks at 1.75×10^5 and 2.77×10^5 Hz, indicating resonance frequencies f_r and f_a, respectively. The k_{33} derived from equation (2) is 80.61% at temperature of 55 ^{o}C.

Figure 7 shows the variation of electromechanical coupling factor as a function of temperature. It can be seen that k_{33} remains at a high value of 78-82% in the

temperature range of 20 °C up to about 80°C. And then suddenly decrease to 51-53% at the temperature range of 90 °C - 125°C, which is believed to result from the rhombohedral-tetragonal phase transition before dropping down at the Curie temperature of 125°C. The k_{33} steeply drops toward zero at above *T*c, which indicates the crystal belong to the paraelectric phase. The piezoelectric coefficient d_{33} was measured to be 1344 pC/N at room temperature using a quasistatic d_{33} meter.

3.4 Ferroelectric properties

The ferroelectric properties of the PYN-PMN-PT(22/44/34) crystals were revealed by the well-developed polarization-electric field hysteresis loops measured at room temperatures, as displayed in Figure 8. The saturation of polarization is achieved at an electric field of ±7 kV/cm and at room temperature. The coercive field *E*c and remnant polarization *P*r are found to be 3.4 kV/cm and 24.1 μC/cm^2, respectively. The coercive field E_C of the PYN-PMN-PT(22/44/34) crystals is higher than that of PMNT crystals, indicating a higher stability for the poled state.

4. Conclusions

The ternary piezoelectric single crystals of PYN-PMN-PT(22/44/34) with dimensions of 26 × 26 × 10 mm^3 have been successfully grown for the first time by the TSSG method, which presents pure perovskite structure. The di-/piezo-/ferroelectric properties of the grown crystals were investigated. The Curie temperature T_C and the rhombohedral-tetragonal phase transition temperature T_{RT}

reached 125 ºC and 90 ºC. The piezoelectric coefficient d_{33} is about 1344 pC/N and the longitudinal electromechanical coupling coefficient k_{33} remains consistently high (78 – 82%) from room temperature up to 80 ^{o}C. The remanent polarization P_r and coercive field E_c were found to be 21.4μC/cm^2, 3.4 kV/cm, for [001]-oriented crystals at room temperature, respectively. These results demonstrate that the PYN-PMN-PT(22/44/34) crystals are a promising candidate for uses in electromechanical transducers for high-power applications. PYN-PMN-PT(22/44/34) crystals are a promising candidate for uses in electromechanical transducers for applications.

Acknowledgments

This work was supported by the Fund of Key Laboratory of Optoelectronic Materials Chemistry and Physics, Chinese Academy of Sciences (2010KL007), the National High Technology Research and Development Program of China (863 Program) under grant No.2011AA030208, the National Natural Science Foundation of China under Grant No. 91122020.

References

1. Z. G. Ye, *Mater. Res. Soc. Bull.* 2009, **34 (4)**, 277.

2. S. E. Park, T. R. Shrout, *J. Appl. Phys.* 1997, **82**, 1804.

3. H. S. Luo, G. S. Xu, P. C. Wang, Z. W. Yin, *Ferroelectrics.* 1999, **231**, 685.

4. M. Dong, Z. G. Ye, *J. Cryst. Growth.* 2000, **209**, 81.

5. A. A. Bokov, Z. G. Ye, *Phys. Rev. B* 2002, **66**, 094112.

6. X. F. Long, Z. G. Ye, *Acta Materialia*. 2007, **55**, 6507.

7. Q. Wan, C. Chen, Y. P. Shen, *J. Mater. Sci.* 2006, **41**, 2993.

8. L.C. Lim, M. Shanthi, K. K. Rajan, C. Y. H. Lim, *J. Cryst. Growth*. 2005, **282**, 330 .

9. G. M. Gehring, W. Z. Chen, Z. G.Ye, G. Shirane, *J. Phys: Condens. Matt*. 2004, **16**, 7113.

10. A. K. A. Slodczyk, Z. Ujma, *J. Cryst. Growth.* 2006, **289**, 134.

11. A. Sehirlioglu, D.A. Payne, P. J. Han, *Appl. Phys*. 2006, **99**, 064101.

12. A. A. Bokov, Z. G. Ye, *J. Mater. Sci.* 2006, **41**, 31.

13. B. Noheda, D.E. Cox, G. Shirane, J. Gao, Z. G. Ye, *Phys. Rev. B*. 2002, **66**, 054104.

14. M. Alguero, A. Moure, L. Pardo, J. Holc, M. Kosec, *Acta Materialia.* 2006, **54**, 501.

15. Z. Kutnjak, J. Petzelt, R. Blinc, *Nature*. 2006, **441**, 956.

16. B. Noheda, D.E. Cox, G. Shirane, J. Gao and Z.-G. Ye, *Phys. Rev. B*, 2002**, 66**, 054104.

17. J. Kuwata, K. Uchino and S. Nomura, *Ferroelectrics*, 1981**, 37**, 579.

18. C. He, X. Z. Li, Z. J. Wang, X. F. Long, S. Y. Mao, and Z. G. Ye, *Chemicals of Materials*, 2010, **22(19)**, 5588.

19. C. He, X. Z. Li, Z. J. Wang, Y. Liu, D. Q. Shen, T. Li,X. F. Long, CrysEngComm, 2012, **14**, 4513.

20. Y. Guo, H. Xu, H. Luo, Z. Yin, *J. Cryst. Growth,* 2001, **226**, 111.

21. Y. Hosono, Y. Yamashita, H. Sakamoto, N. Ichinose, *Jpn. J. Appl. Phys.* 2003, **42**, 5681.

22. S. J. Zhang, J. Luo, W. Hackenberger, N. P. Sherlock, R. J. Meyer, Jr. T. R. Shrout, *J. Appl. Phys.Control*. 2009, **105**, 104506.

23. G. S. Xu, K. Chen, D. F. Yang, J. B. Li, *Appl. Phys. Lett.* 2007, **90**, 032901.

24. P. Yu, F. F. Wang, D. Zhou, W. W. Ge, X. Y. Zhao, H. S. Luo, J. L. Sun, X. J. Meng, J. H. Chu, *Appl. Phys. Lett*. 2008, **92**, 252907.

25. S. J. Zhang, J. Luo, W. Hackenberger, T. R. Shrout, *J. Appl. Phys.Control.* 2008, **104**, 064106.

26. A. N. Salak, N. P. Vyshako, V. M. Ferreira, N. M. Olekhnovich, A. D. Shilin, *Mater. Res. Bull.* 2003, **38**, 453-460.

27. A. N. Salak, A. D. Shilin, M. V. Bushinski, N. M. Olekhnovich, N. P. Vyshako, *Mater. Res. Bull*. 2000, **35**, 1429-1438.

28. W. Qiu, H. H. Hng, *Ceram. Inter.* 2004, **30**, 2171-2176.

29. U.Sukkha, R.Muanghlua, S.Niemchiaroen, B.Boonchom, N.Vittayakorn, *Ferroelectrics*, 2011, **416**, 8-15.

30. Xia Z and Li Q, *Solid State Commun*. 2007, **142**, 323.

31. A. A. Bokov, X. F. Long and Z. G. Ye, *Phys. Rev. B: Condens.Matter,* 2010, **81**, 172103.

32. Z.-G. Ye, *Key Eng. Mater*. 1998, **155**, 81.

33. A. E. Glazounov and A. K. Tagantsev, *Appl. Phys. Lett*. 1998, **73**, 856.

34. D. Viehland, S. J. Jang, L. E. Cross and M. Wuttig, *Phys.Rev. B*, 1992**, 46**, 8003.

35. A. A. Bokov, Y.-H. Bing, W. Chen, Z.-G. Ye, S. A. Bogatina, I. P. Raevski, S. I. Raevskaya, and E.V. Sahkar, *Phys. Rev. B*, 2003, **68**, 052102-1-052102-4.

36. A. A. Bokov and Z.-G. Ye, *Solid State Commun*., 2000, **116**, 105-108.

37. A. A. Bokov and Z.-G. Ye, *Appl. Phys. Lett.,* 2000, **77,** 1888-1890.

38. S. Zhang, C. A. Randall and T. R. Shourt, *J. Appl. Phys.*, 2004**, 95**, 4291.

39. IEEE Standard on Piezoelectricity, *ANSI/IEEE Std.*, 1987**, 176**.

Figure captions

Fig. 1 Photograph of as-grown PYN-PMN-PT(22/44/34) crystals.

Fig. 2 X-ray powder diffraction patterns of the grown PYN-PMN-PT(22/44/34) crystals; (200) reflections composed of one single peak, suggesting rhombohedral symmetry at room temperature as shown in the insets.

Fig. 3 Electric domain micrographs of (001) plate of PYN-PMN-PT(22/44/34) crystal under crossed polar (a) Polarization direction; (b) 45° extinction direction

Fig. 4 Variations of dielectric constant (ε′) and loss tangent (tanδ) of (001)-oriented PYN-PMN-PT(22/44/34) crystals as a function of temperature measured at 1 Hz, 100 Hz, 10K Hz and 1000kHz: (a) unpoled; (b) poled.

Fig. 5 Temperature dependence of 1/ε′ at 1 kHz for the PYN-PMN-PT(22/44/34) crystal; The insets show the fitting to the Lorentz-type quadratic relationship.

Fig. 6 Frequency dependences of the impedance and phase angle of the PYN-PMN-PT(22/44/34) crystals measured at room temperature.

Fig. 7 Temperature dependence of the electromechanical coupling factor k_{33} of a (001)-oriented PYN-PMN-PT(22/44/34) crystal bar.

Fig. 8 Ferroelectric hysteresis loop of (001)-oriented PYN-PMN-PT(22/44/34) single crystals at room temperature.

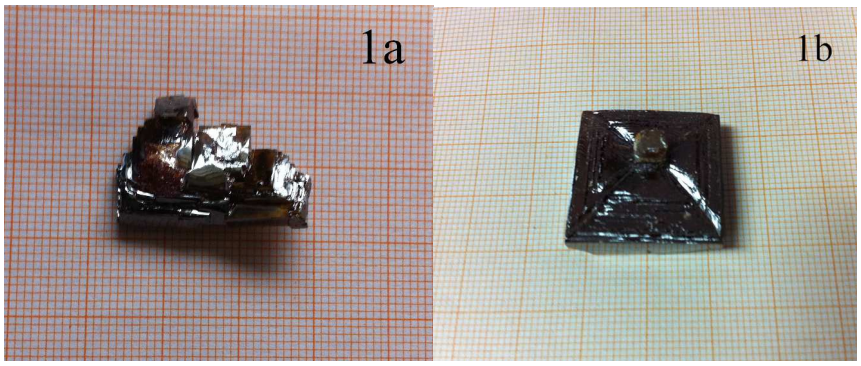

Fig. 1

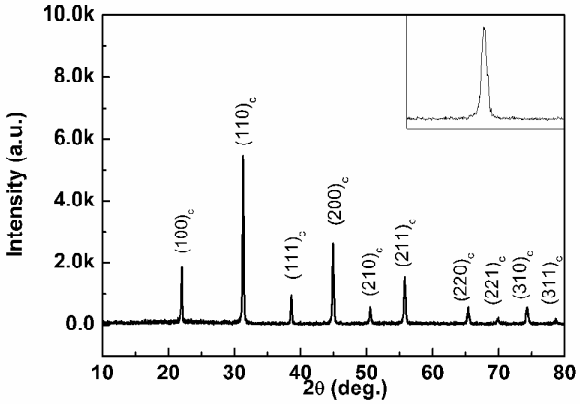

Fig. 2

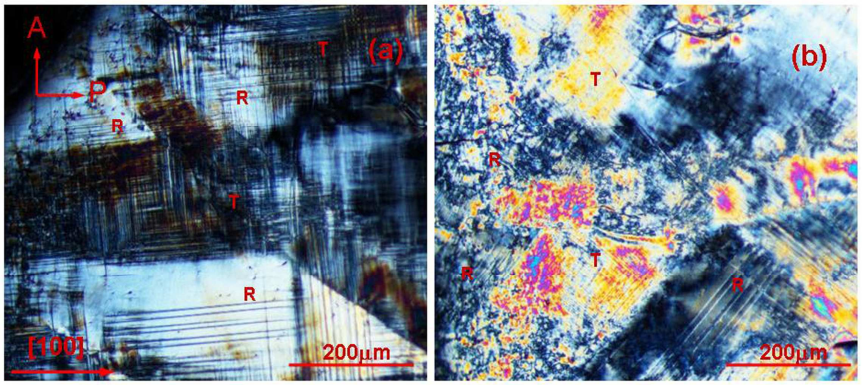

Fig. 3

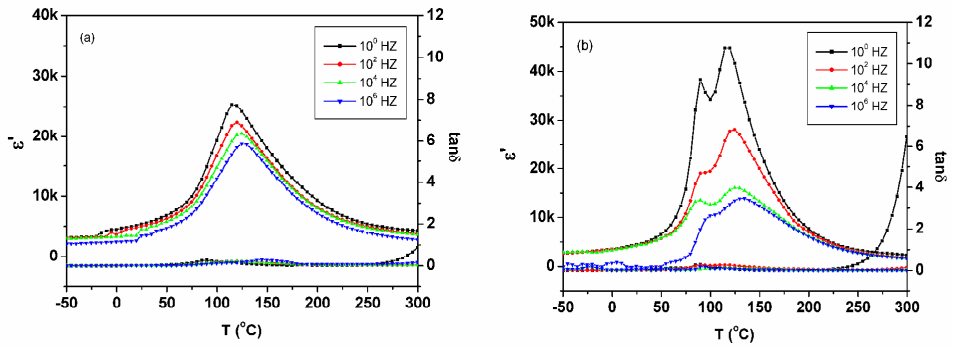

Fig. 4

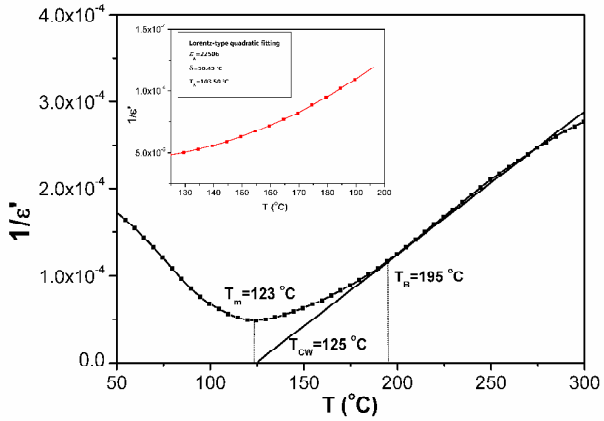

Fig. 5

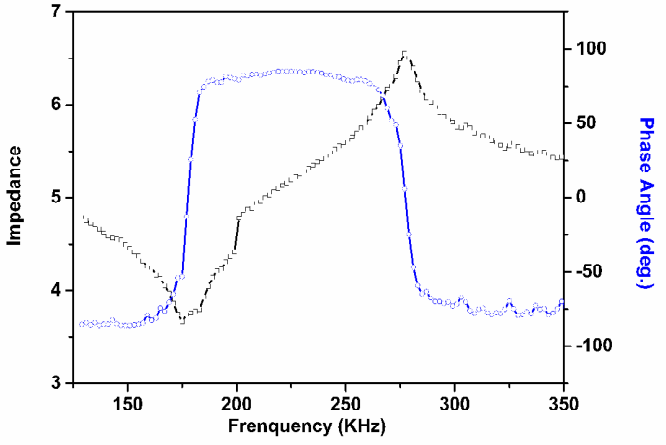

Fig. 6

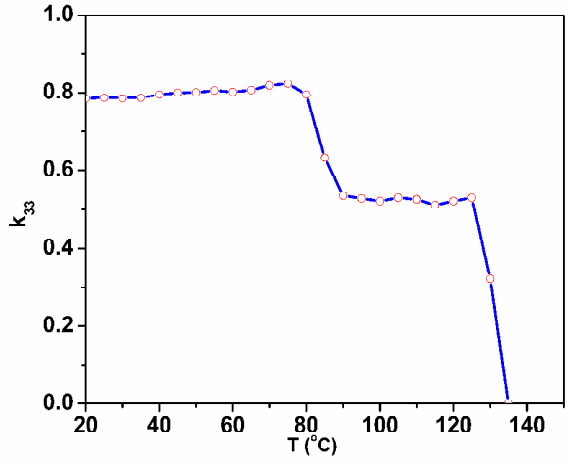

Fig. 7

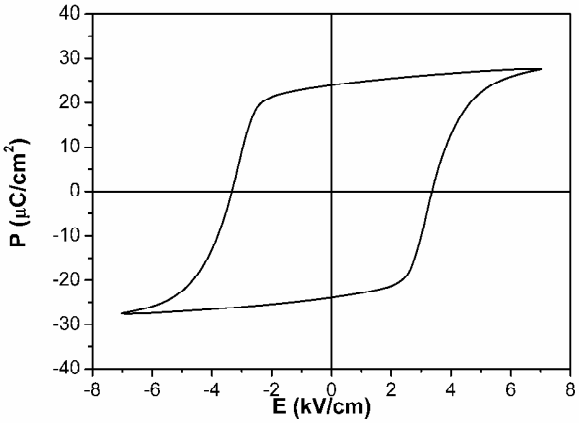

Fig. 8

Abstract

A ternary piezo-/ferroelectric crystal of $0.22Pb(Y_{1/2}Nb_{1/2})O_3$-0.44 $Pb(Mg_{1/3}Nb_{2/3})O_3$-$0.34PbTiO_3$ (PYN-PMN-PT(22/44/34)) with dimensions of 26 × 26 × 10 mm^3 has been grown by the top-seeded solution growth (TSSG) method for the first time with a purpose of exploring new ferroelectric single crystals with high piezoelectric properties, and which was characterized by structural analysis and electrical measurements. The rhombohedral and tetragonal phases co-exist in the as-grown crystals, which belong to the morphotropic phase boundary (MPB) region. The Curie temperature T_C and the rhombohedral-tetragonal phase transition temperature T_{RT} reached 125 ºC and 90 ºC. The dielectric constant ε′, dielectric loss tangent tanδ, piezoelectric coefficient d_{33}, longitudinal electromechanical coupling coefficient k_{33}, remnant polarization P_r and coercive field E_c were found to be 1280 , 0.04, 1344 pC/N, 82%, 21.4μC/cm^2, 3.4 kV/cm, for [001]-oriented crystals at room temperature, respectively. These results show that the PYN-PMN-PT(22/44/34) crystals are a promising candidate for uses in electromechanical transducers for applications.